King Saud University

Arabian Journal of Chemistry

www.ksu.edu.sa
www.sciencedirect.com

ORIGINAL ARTICLE

Electrochemical behavior of PbO$_2$/PbSO$_4$ electrode in the presence of surfactants in electrolyte

O. Saoudi [b], M. Matrakova [c], A. Aleksandrova [c], L. Zerroual [a],*

[a] *Laboratoire d'Energétique et Electrochimie du Solide (LEES), Faculté de Technologie, Université Ferhat ABBAS, Sétif-1 19000, Algeria*
[b] *Laboratoire des Matériaux Inorganiques, Faculté des Sciences, Université de M'sila, 28000 M'sila, Algeria*
[c] *Institute of Electrochemistry and Energy Systems (IEES), Bulgarian Academy of Sciences, Sofia 1113, Bulgaria*

Abstract The electrochemical behavior of PbO$_2$/PbSO$_4$ electrode is investigated in 4.5 M H$_2$SO$_4$ in presence of three surfactants, Sodium Dodecyl Sulfate (SDS), Cetyltrimethylammonium bromide (CTAB) and Sodium tripolyphosphate (STPP), using cyclic voltametry, electrochemical spectroscopy impedance and galvanostatic discharge as techniques. The micro morphology of the surface of the modified PbO$_2$ electrodes is examined by scanning electron microscopy. The results show that SDS and CTAB when added in the electrolyte could refine the coating particles and change the roughness of the surface of the electrode leading to a thin film of PbO$_2$ with amorphous character. In addition, SDS and CTAB shift the hydrogen evolution potential towards more negative values, improve the discharge capacity of the anodic layer and accelerate the charge transfer. Under cathodic polarization, CTAB presents the lowest value of the charge transfer resistance R$_{ct}$. In the contrary, STPP shifts the oxygen evolution potential towards more positive values, passivates the surface of the electrode and inhibits completely the reaction of PbO$_2$ formation.

1. Introduction

The lead/acid battery derives its power from the electrochemical energy released during the conversion of (α- and β-PbO$_2$ to PbSO$_4$, on the positive plate, and Pb to PbSO$_4$, on the negative plate. The major factor contributing to the decline in capacity of the positive plate during charge/discharge cycling was considered to be a progressive decrease in the degree of electrical contact between the PbO$_2$ particles in the plate and between these particles and the grid. The change in conductivity is mainly due to the combined effects of grid corrosion and a gradual softening of the plate mass and shedding of the PbO$_2$ particles. The life of lead acid battery positive plates depends on both grid corrosion and

the softening and shedding of PbO$_2$ active material. During charging, the positive grid of the lead acid battery is oxidized and thus a boundary layer is formed between the grid and the active mass. The growth of the oxide layer is due to the diffusion of oxygen through the layer. Previous works (Pohl and Shendler, 1984; Bullock and Butler, 1986; Pavlov and Mohanov, 1993) proposed different mechanisms. The oxygen generated at the electrolyte interface diffuses into the layer in the form of atoms or radicals and oxidizes the underlying lead to tetragonal PbO which further gives intermediate oxides PbO$_x$ and finally these non-stoichiometric oxides are converted to α-PbO$_2$. The composition of the anodic layer depends on the potential and the quantity of electricity that has passed through the electrode. It has been found that the anodic layer formed after oxidation of Pb-Sb-Sn electrodes contains in addition of tet-PbO and PbO$_2$ substituted oxides. Recently, a new concept has been proposed for the structure of lead dioxide (Mohanov and Pavlov, 1987).

According to this concept, the lead dioxide active mass consists of crystal zones and hydrated zones designated by PbO(OH)$_2$ with amorphous character. The characteristics of the layer have an influence on the cycling behaviour and cycle life of the battery. That is why the growth mechanism and the properties of the boundary layer are of great interest. Since the early start of manufacturing lead/acid cells, the use of additives, and more specifically the selection of these compounds, has been conducted by empirical rules and experience.

During the last decades the lead/acid cell has been the subject of many studies, which have increased enormously the knowledge of the effects of additives and of the manufacturing process. PbO$_2$ electrode is an attractive and promising anode material due to its low cost, ease synthesis, high oxygen evolution potential and corrosion resistance (Liu and Liu, 2008; Tan et al., 2011). In addition of its high electrical performance as positive active material for lead-acid batteries, it exhibits a strong mineralization capacity for recalcitrant organic compounds. The effect of some additives on the capacity of the PbO$_2$ electrode and its efficiency in wastewater treatment was widely investigated in the literature (Comninellis, 1994; Panizza and Cerisola, 2009; Niu et al.2016; Xiaoliang et al., 2017; Boudieb et al., 2015).

In a previous work (Ghaemi et al., 2006) demonstrated that the nonionic surfactant t-octyl phenoxy polyethoxyethanol (Triton X-100) improves the charge/discharge of the modified PbO$_2$ electrode and increases the overpotential for oxygen evolution. (Darabizad et al., 2015) synthesized nanostructured PbO$_2$ by electrodeposition at constant current on Ti substrate in presence of polyvinylpyrrolidone (PVP). The results revealed that the particle size and morphology of PbO$_2$ can be controlled by altering PVP concentration. In addition, the charge transfer resistance significantly decreased in the presence of PVP. In their study on the effects of surfactants on sulfation of negative active material in lead acid battery under PSOC condition (Ghavami et al., 2016) showed that amongst all tested surfactants, the cell with anionic sodium dodecyl sulfate surfactant (SDS) exhibits the longest cycle life with the least overcharge and fine PbSO$_4$ crystals but the cell with cationic cethyl trimethyl ammonium bromide (CTAB) surfactant shows opposite effects. (Boudieb et al., 2016) published a paper on the effect of a phosphonate surfactant (PS) on the electrochemical behavior of the lead-acid battery positive plate and concluded that the use of surfactant at low concentration substantially changes the morphology of the lead sulfate crystals and increases the capacity and cycle life of the positive plate. Recently, Fu et al. (2018) prepared various structured PbO$_2$ thin-film electrodes by surfactant assisted anodic electro-deposition method. The electrochemical performance of PbO$_2$ electrodes was found to be strongly dependant on their morphology and structure. Compared to other structures studied, PbO$_2$-PEG electrode shows excellent electrocatalytic activity, stability, and service life. Similarly, Duan et al. (2018) fabricated a hydrophobic PbO$_2$ electrode modified by sodium dodecyl benzene sulfonate (SDBS-PbO$_2$) and tested it as anode for electrochemical degradation of nitrobenzene in aqueous solution. The results showed that the electro-catalytic activity for nitrobenzene degradation obtained with SDBS-PbO$_2$ electrode was much higher than that of pure PbO$_2$ electrode.

In the present work, different structured PbO$_2$ electrodes were prepared by surfactant-assisted anodic polarization method. We investigated the effect of SDS, CTAB and STPP as surfactants added in the electrolyte (4.5 M H$_2$SO$_4$) on the electrochemical behavior of Pb-Sb-Sn alloy. Cyclic voltametry, electrochemical spectroscopy impedance and galvanostatic discharge were used as techniques. The effect of the surfactants on the micro morphology of the surface and structure of the modified PbO$_2$ electrodes were examined by scanning electron microscopy.

2. Experimental

The working electrode, a Pb-Sb-Sn alloy, was polished with emery paper (600, 800, 1200 mesh) under water and etched with a mixture (80% CH$_3$COOH and 20% H$_2$O$_2$). Cleaning was done by shaking the electrode for approximately 20 s. Afterwards, the working electrode was rinsed with double-distilled water and ethanol. This procedure was repeated until the electrode appeared shiny. The electrochemical behavior of Pb-Sb-Sn alloy in 4.5 M H$_2$SO$_4$ containing SDS (0.12), CTAB (0.024), and STPP (1.20%), was investigated using cyclic voltammetry. After a rest of 1 min in the electrolyte, the electrodes were cathodically polarized at -1.3 V for 30 min then anodically polarized at 1.7 V for another 30 min. Cyclic voltammograms were obtained up to 100 cycles between 0.7 and 1.7 V versus Hg/Hg$_2$SO$_4$ reference electrode at a sweep rate of 10 mV·s^{-1}. The potential current density curves were recorded. The capacity expressed in mAh·cm^{-2} is determined by integrating the surface area of the cathodic peak corresponding to the reduction of PbO$_2$ to PbSO$_4$. Impedance measurements were performed in the frequency range from10 mHz to 100 kHz at a signal amplitude of 10 mV. The impedance spectra of pure and modified PbO$_2$ electrodes were recorded at open circuit potential (1077 mV) and under cathodic polarization (1050, 850 and 750 mV). The charge transfer resistance was plotted against the cathodic polarization value. A thin layer of PbO$_2$ was formed after polarization of each electrode at 1.7 V for 30 min and the micro morphology and crystal structure of the electrodes were characterized by scanning electron microscopy (SEM, JEOL, JSM-6390A).

The different electrodes were then discharged at a constant cathodic current of 1 mA, the potential-time curves were recorded using Hg/Hg$_2$SO$_4$/saturated K$_2$SO$_4$ reference electrode. All experiments were carried out at room temperature.

3. Results and discussion

3.1. Oxygen evolution

Fig. 1 shows the linear sweep voltammetry of Pb-Sb-Sn alloy in 4.5 M H$_2$SO$_4$ in the range potential of oxygen evolution in presence and absence of the three surfactants. During the potential sweep, we observe an increase in the current density and the appearance of an anodic peak at 1.42 V corresponding to the oxidation of PbSO$_4$ to PbO$_2$. The presence of SDS and CTAB in the electrolyte compared to the blank test seems to facilitate the oxidation reaction of lead sulfate crystals with a slight shift of oxygen evolution potential towards negative values. In contrast, when STPP is added to the solution, a low and constant current density is recorded. The STPP covers the sur-
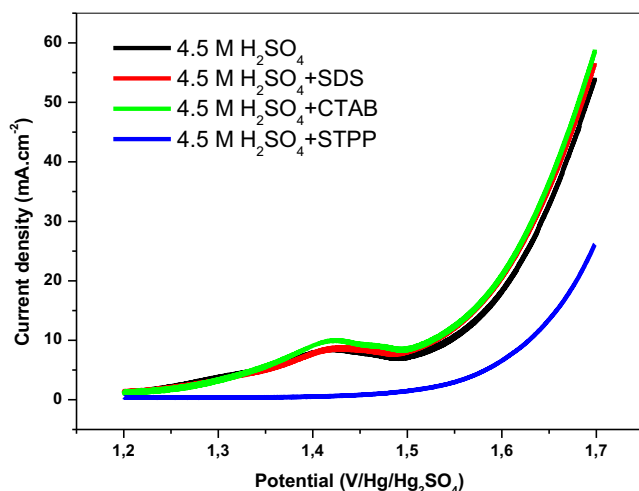
Fig. 1 Linear sweep voltammograms of Pb-Sb-Sn alloy at a sweep rate of 50 mV·s^{-1} in 4.5 M H$_2$SO$_4$ without and with SDS, CTAB and STPP as additives (anodic polarization).

face of the electrode with a passive film and inhibits completely the oxidation reaction of PbSO$_4$ crystals with a shift of oxygen evolution potential towards more positive values.

3.2. Hydrogen evolution

Fig. 2 illustrates the linear sweep voltammetry of Pb-Sb-Sn alloy in 4.5 M H$_2$SO$_4$ in the range potential of hydrogen evolution in presence and absence of the three surfactants. During the potential sweep, we record a progressive increase in the current density at −1.4 V. This is followed by an important gasing due to the hydrogen evolution at the surface of the electrode. The hydrogen evolution potential is shifted to more negative values when SDS and CTAB are present in the
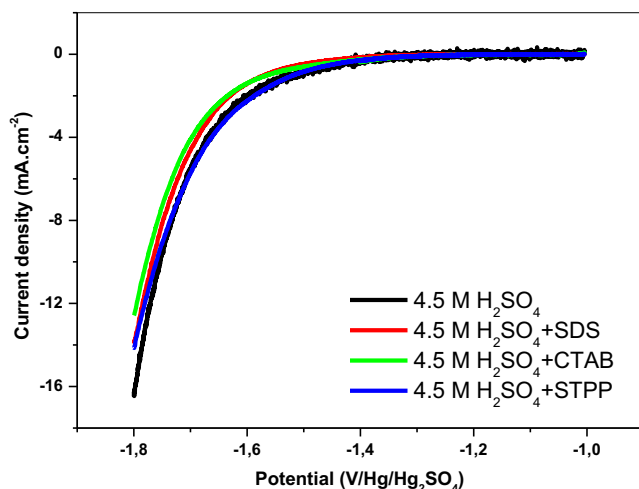

Fig. 2 Linear sweep voltammograms of Pb-Sb-Sn alloy at a sweep rate of 50 mV·s^{-1} in 4.5 M H$_2$SO$_4$ without and with SDS, CTAB and STPP as additives (cathodic polarization).

electrolyte. In fact surfactants may strongly adsorb, suppress and/or modify the structure of the electrode so that its surface may be less accessible to water molecules and water and/or protons discharge is inhibited. Consequently, both oxygen and hydrogen evolutions at the positive and negative electrode are respectively shifted to more positive and negative potentials. As STPP does not influence the reduction of H$^+$ and inhibits the oxidation of PbSO$_4$, the study is restricted to CTAB and SDS.

3.3. Micro morphology of PbO$_2$ electrodes

Fig. 3 shows the SEM images of the different PbO$_2$ electrodes. From Fig. 3a, it could be observed that the morphology of PbO$_2$ electrode was coarse and uneven. Typical crystalline structures were observed on the electrode surface. Larger and clearly pronounced individual PbO$_2$ particles with a number of micro-pores are grouped in small agglomerates, which coalesce into an aggregate. As shown in Fig. 3b and c, smaller and closer interconnected PbO$_2$ particles in agglomerates with individual nanosized particles still distinguished are observed in the SEM images of the modified PbO$_2$ electrodes after addition of SDS and CTAB. The surfactants change the roughness of PbO$_2$ films, consequently smooth and hydrated layers with amorphous structure are obtained in presence of SDS and CTAB as additives in H$_2$SO$_4$ solutions.

3.4. Cyclic voltammetry

The cyclic voltammetry of Pb-Sb-Sn alloy electrode in 4.5 M H$_2$SO$_4$ performed in the potential range (1.5–0.5 V vs Hg/Hg$_2$-SO$_4$/K$_2$SO$_4$ reference electrode), in presence and absence of the different surfactants, are presented in Fig. 4. Both SDS and CTAB present almost the same voltammograms as that of the blank test (see Fig. 4a). During discharge, we observe a cathodic peak at around 1 V which corresponds to the reduction of PbO$_2$ to PbSO$_4$. The peak current density increases with the increase of the cycle number. High current densities are recorded for the solutions containing respectively SDS and CTAB (see Fig. 4a and b). The capacity versus the number of cycles for the different electrodes is illustrated in Fig. 4d. We can see that the increase in capacity for PbO$_2$ prepared in presence of SDS and CTAB respectively is more important compared to that of the blank test. Consequently the presence of the surfactants in the electrolyte seems to facilitate the production of active PbO$_2$. In the anodic branch, it is clearly seen that the peak that corresponds to the oxidation of PbSO$_4$ to PbO$_2$ is completely masked by oxygen evolution.

3.5. Electrochemical impedance spectroscopy

The Nyquist plots of the impedance at open circuit potential (OCP) and under cathodic polarization of Pb-Sb-Sn alloy in the different electrolytes are shown in Fig. 5. They consist of a semicircle and a straight line. The semicircle is related to charge transfer resistance and double layer capacitance formation. It can be observed that the diameter of semicircle that is related to charge transfer resistance, and capacitance value are increased with the increase of the cathodic polarization (see Fig. 5a–d). Fig. 6 represents the variation of the charge transfer resistance with the cathodic polarization applied to PbO$_2$
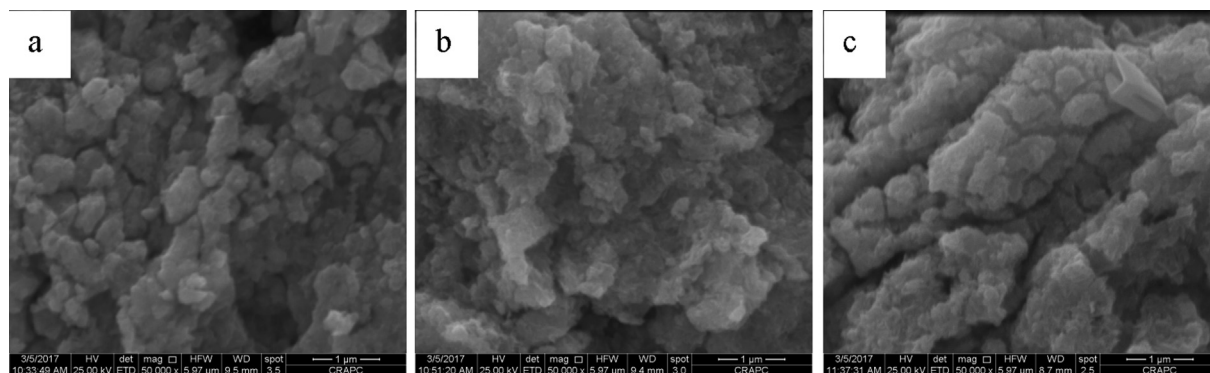
Fig. 3 SEM images of the different PbO₂ electrodes obtained after anodic polarization of Pb-Sb-Sn alloy in: (a) 4.5 M H₂SO₄, (b) 4.5 M H₂SO₄ + SDS, (c) 4.5 M H₂SO₄ + CTAB.
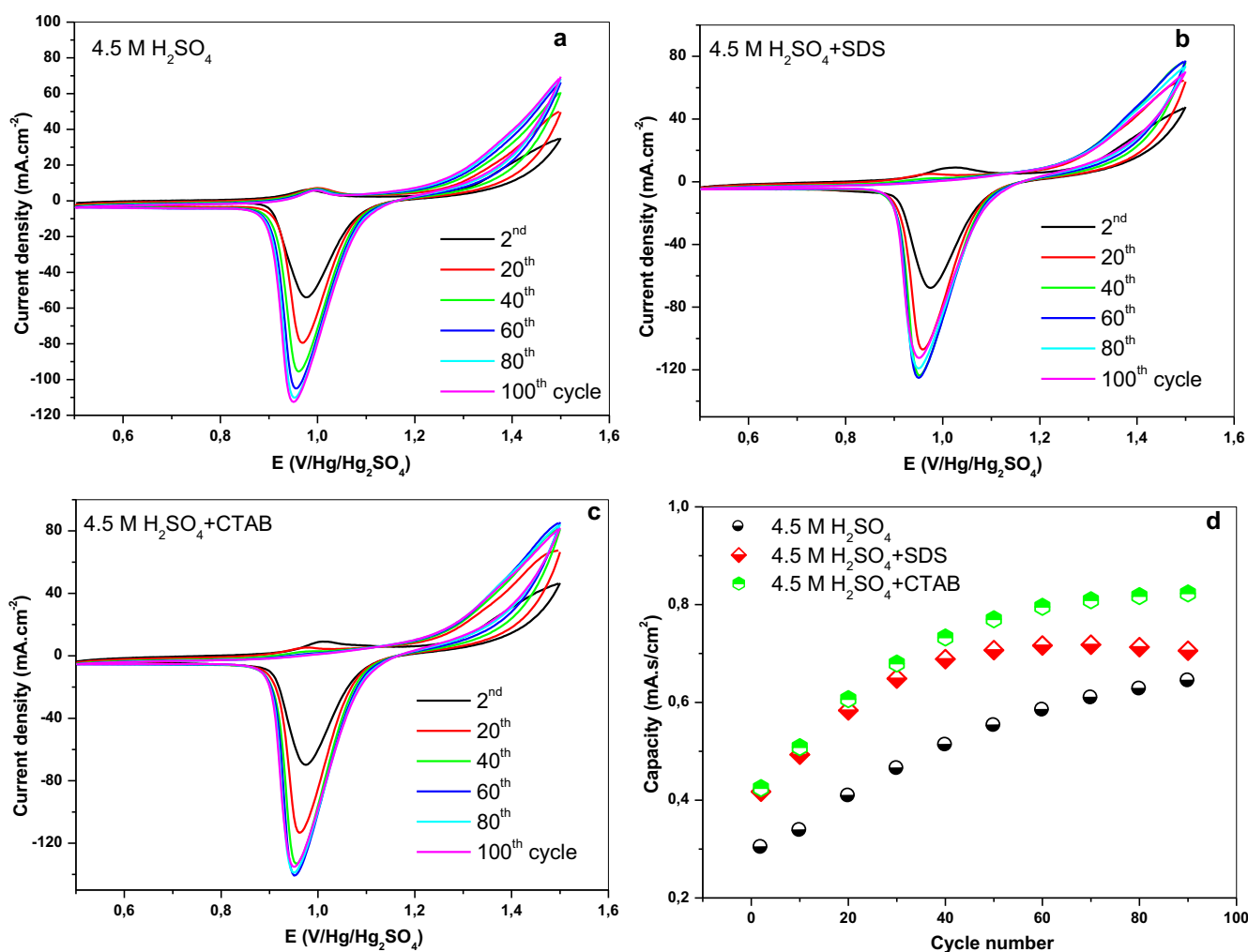

Fig. 4 Cyclic voltammograms of Pb-Sb-Sn alloys at a sweep rate of 10 mV·s⁻¹ in: (a) 4.5 M H₂SO₄, (b) 4.5 M H₂SO₄ + SDS, (c) 4.5 M H₂SO₄ + CTAB, and (d) discharge capacity versus cycle number.

prepared in presence and absence of SDS and CTAB as additives to H₂SO₄ solution. The different electrodes show an increase of the charge transfer resistance with the increase of the overpotential value. This could be explained by the fact that under polarization amorphous particles of PbO₂ are partially converted to PbSO₄ leading to higher resistance. Small values of charge transfer resistance are obtained when SDS and CTAB are added to H₂SO₄ solution.
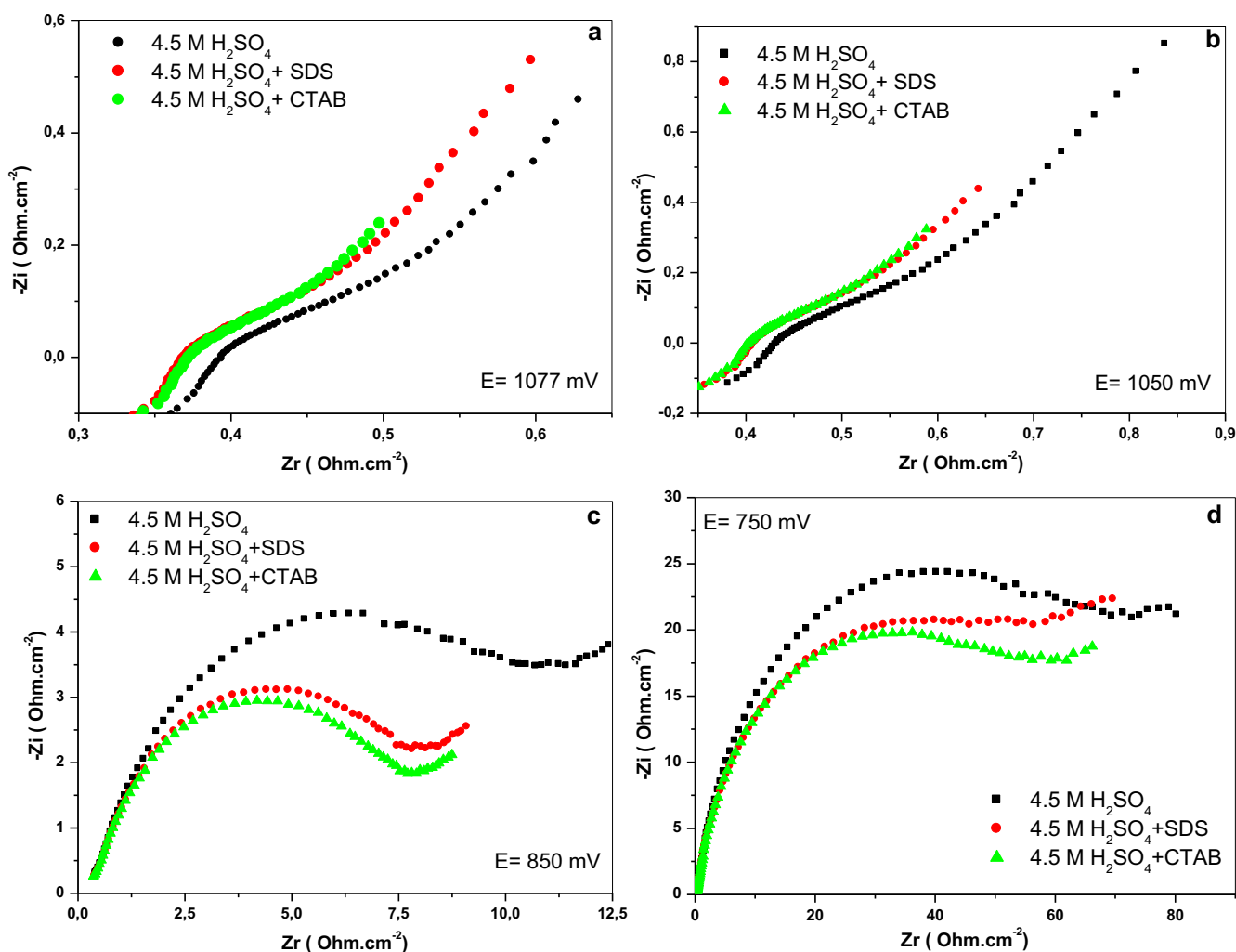
Fig. 5 Nyquist plots of the different PbO$_2$ electrodes in 4.5 M H$_2$SO$_4$: (a) E = 1077 mV, (b) E = 1050 mV, (c) E = 850 mV, (d) E = 750 mV.
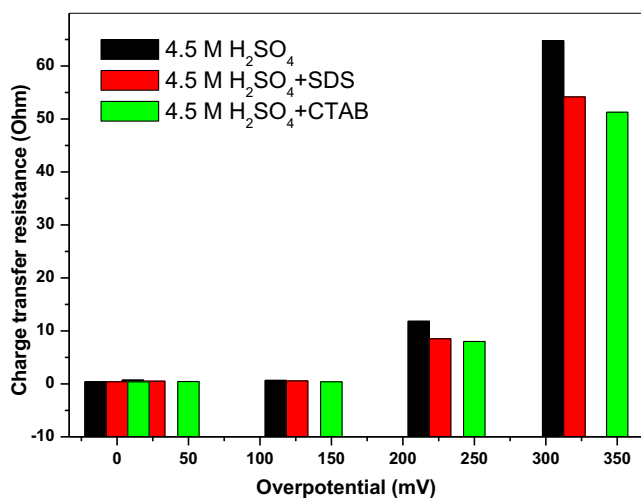

Fig. 6 Variation of the charge transfer resistance of the different PbO$_2$ electrodes in 4.5 M H$_2$SO$_4$ with overpotential.

3.6. Galvanostatic discharge

The discharge curves of thin layers of PbO$_2$ formed after polarization of the electrodes at 1.7 V for 30 min in electrolytes containing SDS and CTAB as additives are compared in Fig. 7. We report the change in potential versus discharge time expressed in seconds. We can see that PbO$_2$ formed in H$_2$SO$_4$ solutions containing SDS and CTAB presents an open circuit potential slightly higher than that of PbO$_2$ prepared in absence of additives. Consequently, this yields to a potential plateau that corresponds to the reduction of PbO$_2$ to PbSO$_4$ slightly higher. We notice that the discharge times recorded for the thin layers of PbO$_2$ formed in H$_2$SO$_4$ solutions containing SDS and CTAB are much higher than that of the blank test (i.e. PbO$_2$ obtained in H$_2$SO$_4$ solutions without additives). This is due to the amorphous structure of PbO$_2$ layers as clearly shown by the SEM images of the modified electrodes.
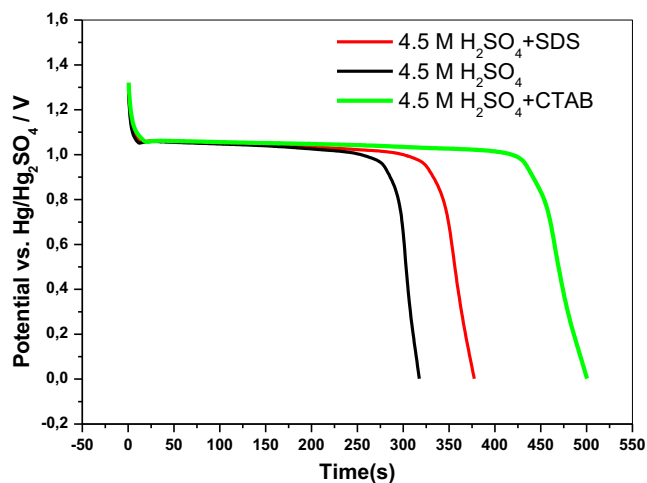
Fig. 7 Galvanostatic discharge curves of the different PbO$_2$ electrodes in 4.5 M H$_2$SO$_4$.

4. Conclusion

The study of the behavior of Pb-Sb-Sn alloys in 4.5 M H$_2$SO$_4$ in presence of three surfactants SDS, CTAB, and STPP are carried out. The electrodes are anodically polarized to form thin layers of PbO$_2$. The morphology and electrochemical properties of the prepared PbO$_2$ electrodes are characterized to investigate the effects of the surfactants when added in H$_2$SO$_4$ solutions. The examination of the surface of the PbO$_2$ modified electrodes shows that in presence of SDS and CTAB smooth thin films of PbO$_2$ with amorphous character are obtained. The experimental results show among these surfactants STPP inhibits completely the reaction of the formation of the anodic layer of PbO$_2$. In addition, it does not affect the discharge of H$^+$. Whereas CTAB seems to improve its discharge capacity, electrical performance and increase hydrogen evolution potential. Under cathodic

polarization, low value of charge transfer resistance is obtained in presence of this additive. Further investigations on lead-acid battery pastes are in progress to understand this controversy between the different surfactants.

Declaration of Competing Interest

The authors declare that they have no known competing financial interests or personal relationships that could have appeared to influence the work reported in this paper.

References

Boudieb, N., Bounoughaz, M., Bouklachi, A., 2015. Proc. – Soc. Behav. Sci. 195, 1618.

Boudieb, N., Bounoughaz, M., Bouklachi, A., 2016. Int. J. Electrochem. Sci. 11, 215.

Bullock, K.R., Butler, M.A., 1986. J. Electrochem. Soc. 133, 1085.

Comninellis, C., 1994. Electrochim. Acta 39, 1857.

Darabizad, G., Rahmanifar, M.S., Mousavi, M.F., Pendashteh, A., 2015. Mater. Chem. Phys. 156, 121.

Duan, X., Xu, F., Wang, Y., Chen, Y., Chang, L., 2018. Electrochim. Acta 282, 662.

Fu, F., Yang, W., Ke, C., 2018. Mater. Chem. Phys. 220, 155.

Ghaemi, M.E., Ghafouri, M., Neshati, J., 2006. J. Power Sources 157, 550.

Ghavami, R.K., Kameli, F., Shirojan, A., Azizi, A., 2016. J. Storage Mater. 7, 121.

Liu, Y., Liu, H., 2008. Electrochim. Acta 53, 5077.

Monahov, B., Pavlov, D., 1987. J. Appl. Electrochem. 218, 135.

Niu, J., Li, Y., Shang, E., Xu, Z., Liu, J., 2016. Chemosphere 146, 526.

Panizza, M., Cerisola, G., 2009. Chem. Rev. 109, 6541.

Pavlov, D., Mohanov, B., 1993. J. Electroanal. Chem. 23, 1244.

Pohl, J.P., Shendler, W., 1984. J. Power Sources 13 (101).

Tan, C., Xiang, B., Li, Y., Fang, J., Huang, M., 2011. Chem. Eng. J. 166, 15.

Xiaoliang, Li, Hao, Xu, Wei, Yan, 2017. J. Alloy. Compd. 718, 386.